Electrocatalysis

International Edition: DOI: 10.1002/anie.201903200
German Edition: DOI: 10.1002/ange.201903200

Oxygen Isotope Labeling Experiments Reveal Different Reaction Sites for the Oxygen Evolution Reaction on Nickel and Nickel Iron Oxides

*Seunghwa Lee, Karla Banjac, Magalí Lingenfelder, and Xile Hu**

Abstract: *Nickel iron oxide is considered a benchmark non-precious catalyst for the oxygen evolution reaction (OER). However, the nature of the active site in nickel iron oxide is heavily debated. Here we report direct spectroscopic evidence for the different active sites in Fe-free and Fe-containing Ni oxides. Ultrathin layered double hydroxides (LDHs) were used as defined samples of metal oxide catalysts, and ^{18}O-labeling experiments in combination with in situ Raman spectroscopy were employed to probe the role of lattice oxygen as well as an active oxygen species, $NiOO^-$, in the catalysts. Our data show that lattice oxygen is involved in the OER for Ni and NiCo LDHs, but not for NiFe and NiCoFe LDHs. Moreover, $NiOO^-$ is a precursor to oxygen for Ni and NiCo LDHs, but not for NiFe and NiCoFe LDHs. These data indicate that bulk Ni sites in Ni and NiCo oxides are active and evolve oxygen via a $NiOO^-$ precursor. Fe incorporation not only dramatically increases the activity, but also changes the nature of the active sites.*

Electrochemical water splitting provides a convenient means to store renewable electricity generated by solar and wind farms in the form of hydrogen fuel. The oxygen evolution reaction (OER) is the efficiency-limiting half reaction of water splitting. Significant research effort has recently been invested in the development of efficient and Earth-abundant electrocatalysts for the OER.[1] Nickel oxides (NiO_xH_y) have long been studied as OER catalysts in alkaline medium.[2] Doping of NiO_xH_y with Fe increases the activity of the former by up to 1000-fold,[3] and the resulting NiFe oxide catalyst ($NiFeO_xH_y$) is considered the benchmark OER catalyst.[4] Although the activity of $NiFeO_xH_y$ is well-established, the fundamental aspects of this catalyst, notable the nature of the active site, are unresolved and the subject of intense debate.[1,3b,4d,5] A growing number of density functional theory computations, spectroscopic investigations, and electrochemical studies argue for Fe to be the active metal,[5c,h,6] while evidence is also presented to support Ni as the active metal.[5d,e,g,7] An important experimental result consistent with Ni being the active site is the observation of $NiOO^-$ (described as adsorbed "active oxygen") species by in situ Raman spectroscopy in both NiO_xH_y[7] and $NiFeO_xH_y$[5d] catalysts. This observation has not been reconciled in mechanistic proposals favoring Fe active sites. By combining ^{18}O-labeling experiments with in situ Raman spectroscopy, we find that $NiOO^-$ species in Fe-free Ni and NiCo oxides can exchange with OH^- from the electrolyte and are precursors to dioxygen. In contrast, upon incorporation of Fe, $NiOO^-$ species cannot exchange with OH^- from the electrolyte and are not precursors to dioxygen. Moreover, lattice oxygen is involved in the OER for Ni and NiCo oxides,[8] but not for NiFe and NiCoFe oxides.[9] These results provide direct experimental evidence for different active sites in Ni and NiFe oxides, thus offering new insights into the mechanism of the OER by the benchmark $NiFeO_xH_y$ catalyst.

We used ultrathin layered double hydroxide (LDH) nanosheets as samples of Ni, NiCo, and NiFe oxides for the following reasons: 1) Although metal oxides can exist in various forms, including as LDHs, the active forms of these oxides in the OER have structures similar to LDHs; 2) LDHs have a uniform and defined bulk composition which simplifies spectroscopic analysis; 3) ultrathin LDH nanosheets are thicker than surface layers of metal oxides, thus representing bulk samples. On the other hand, the ultrasmall thickness may allow a complete exchange of bulk lattice atoms if the exchange is to happen. The ultrathin Ni, NiCo (25% Co), and NiFe (25% Fe) LDHs were synthesized by modifying a method previously developed for the synthesis of MgAl LDH nanosheets.[10] The samples were characterized by inductively coupled plasma-optical emission spectrometry (ICP-OES, Table S1), transmission electron microscopy (TEM), and atomic force microscopy (AFM; Figures S1 and S2). Representative TEM images show that the samples consist of nanosheets with diameters of 10–50 nm. The nanosheets have a faint contrast, consistent with their ultrathin nature. The height profiles acquired by AFM indicate that they are about 1.5–2.0 nm thick. The nanosheets were drop-casted on a gold substrate that was electrochemically roughened for subsequent in situ Raman spectroscopic analysis.[5d] Experiments were conducted using a custom-made in situ electrochemical-Raman cell (Figure S3) in 0.1M Fe-

[*] Dr. S. Lee, Prof. Dr. X. L. Hu
Laboratory of Inorganic Synthesis and Catalysis
Institute of Chemical Sciences and Engineering
Ecole Polytechnique Fédérale de Lausanne (EPFL)
1015 Lausanne (Switzerland)
E-mail: xile.hu@epfl.ch
Homepage: http://lsci.epfl.ch
K. Banjac, Dr. M. Lingenfelder
Max Planck-EPFL Laboratory for Molecular Nanoscience and Technology and Institute of Physics
Ecole Polytechnique Fédérale de Lausanne (EPFL)
1015 Lausanne (Switzerland)
Supporting information and the ORCID identification number for two of the authors of this article can be found under: https://doi.org/10.1002/anie.201903200.

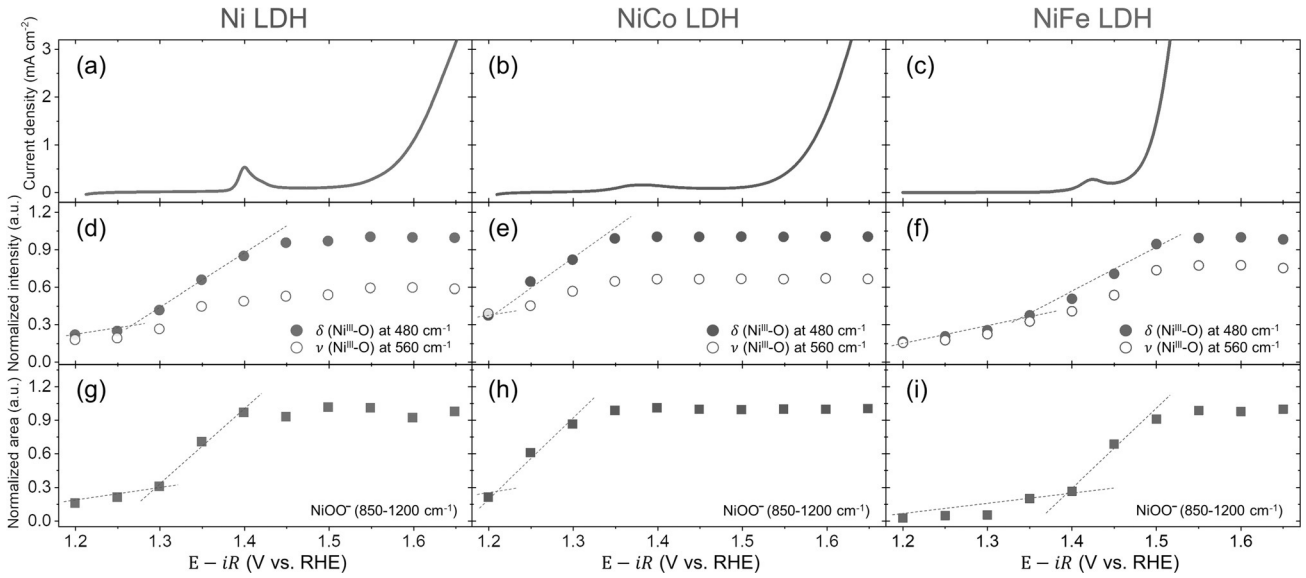

Figure 1. In situ Raman characterization. a–c) LSV curves of Ni, NiCo, and NiFe LDH nanosheets measured at a scan rate of 1 mV s^{-1} in 0.1 M Fe-free KOH; d–f) normalized peak intensities at 480 and 560 cm^{-1} of in situ Raman spectra of each catalyst; g–i) normalized peak areas between 850 and 1200 cm^{-1} arising from the active oxygen species of each catalyst.

free KOH solutions (to avoid Fe contamination). Control experiments confirmed the innocent nature of the gold substrate in the OER and Raman measurements (Figure S4). Moreover, extended exposure of the LDH samples to the Raman laser caused no obvious phase change (Figure S5).

The electrochemical behavior of the Ni, NiCo, and NiFe LDHs (Figure 1 a–c) is consistent with literature reports of Ni, NiCo, and NiFe oxides.[4c,11] In the linear-sweep voltammogram (LSV) of Ni LDH (Figure 1 a), the oxidation of $Ni(OH)_2$ to NiOOH was observed at 1.4 V versus RHE, and the apparent OER took place from 1.55 V. The oxidation of Ni was shifted toward a lower potential in NiCo LDH, while this oxidation was partially suppressed in NiFe LDH (Figure 1 b,c). Incorporation of Co and Fe, especially of Fe, significantly increased the OER activity (Figure 1 a–c and Figure S6), again consistent with previous reports.[3b,4c,11]

In situ Raman experiments revealed Raman peaks corresponding to $\delta(Ni^{III}–O)$ (480 cm^{-1}) and $\nu(Ni^{III}–O)$ (560 cm^{-1}) upon formation of NiOOH[3a,5d,7] at sufficiently positive potentials for all three catalysts (Figure S7). Similar results were obtained under constant current densities (3–10 mA cm^{-2}, Figure S8).

A broad feature previously assigned to ν(O–O) of an active oxygen species $NiOO^-$[5d,7,12] was also observed in the region of 850–1200 cm^{-1} for all the samples (Figure S7). As reported previously,[5d,7] the peak position and its isotopic shift (see below) correspond to a superoxo species ($NiOO^-$) rather than an oxide (NiO^-). The potential-dependent intensities of these peaks are shown in Figure 1 d–i. The intensities of $\delta(Ni^{III}–O)$ and $\nu(Ni^{III}–O)$ reach maximum, steady-state values at potentials just beyond the oxidation of $Ni(OH)_2$ to NiOOH. The signals from $NiOO^-$ appear in a nearly synchronized manner to those of $Ni^{III}–O$, similar to previous reports.[5d,7] Although the mechanism for the formation of $NiOO^-$ remains unclear, it has been proposed that redox-active oxygen species (O(−1) or O(0)) might be formed upon oxidation of $Ni(OH)_2$ to NiOOH.[12] These oxygen species might form an O–O bond, thereby leading to the observed $NiOO^-$. Our data are consistent with this hypothesis.

Isotope labeling experiments were conducted in a three-step approach (Figure 2). First, oxygen atoms in the LDH samples (in the form of $Ni(OH)_2$ and its doped versions) were labeled with ^{18}O by conducting the OER at 1.65 V for 3 min in 0.1 M solutions of $K^{18}OH$ in Fe-free $H_2{}^{18}O$. After this process, the $\delta(Ni^{III}–O)$ (480 cm^{-1}) and $\nu(Ni^{III}–O)$ (560 cm^{-1}) peaks of all the samples were shifted by 25 cm^{-1} to lower frequencies (Figure 3), consistent with the ^{18}O labeling of lattice O atoms. The ν(O–O) band of $NiOO^-$ was shifted by about 50 cm^{-1}, also consistent with successful O^{18} labeling of this moiety. The ^{18}O-labeled catalysts (now in the form of NiOOH and its doped versions) were then immediately placed back (within 30 s) in 0.1 M solutions of $K^{16}OH$ in Fe-free $H_2{}^{16}O$ (Step II).

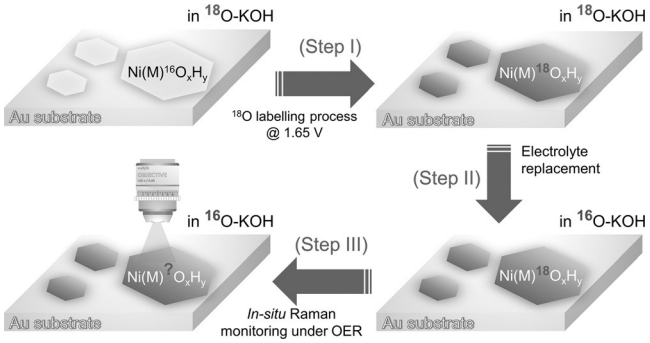

Figure 2. A three-step procedure for the oxygen isotope labeling experiments. Step I is the labeling process of the catalyst with ^{18}O in 0.1 M ^{18}O-KOH by applying a potential of 1.65 V. The electrolyte is then replaced with ^{16}O-KOH (step II). In the last step, the Raman spectrum is recorded in situ at a constant potential of 1.65 V. M = Ni, Co, or Fe.

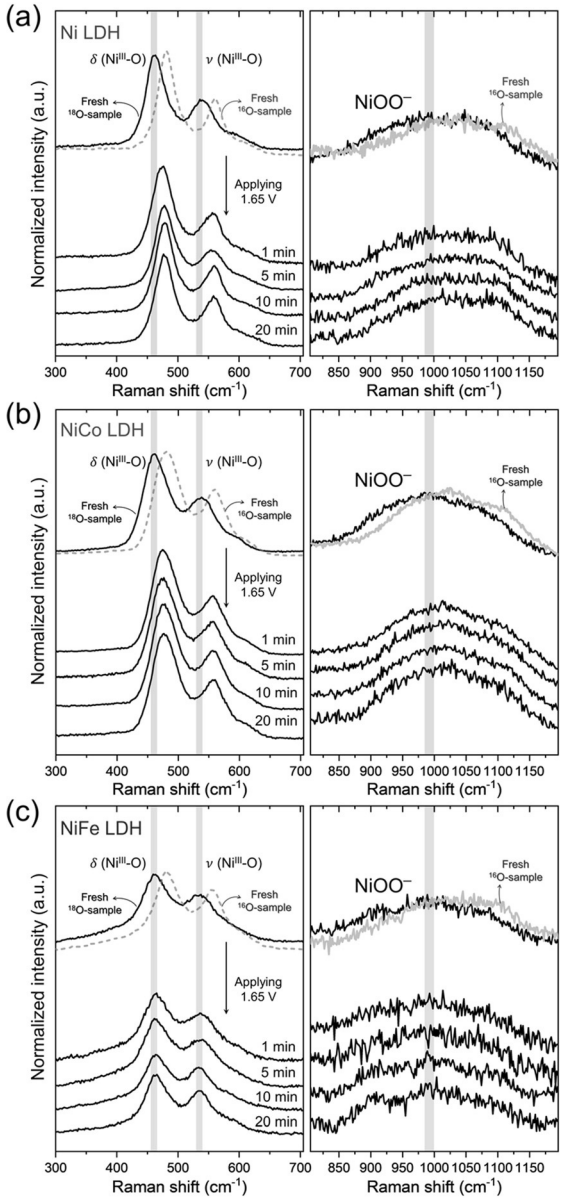

Figure 3. Isotope exchange experiments. In situ Raman spectra of ^{18}O-labeled a) Ni, b) NiCo, and c) NiFe LDHs measured at 1.65 V in 0.1 M KOH in $H_2{}^{16}O$. The Raman spectra were obtained in the regions of the Ni species, such as NiOOH (left column) and $NiOO^-$ (right column). For ease of comparison of peak shift arising from the ^{18}O-labeling process, ^{16}O-labeled peaks of each catalyst are indicated on the right-hand side of peaks corresponding to the as-prepared samples labeled by ^{18}O.

Figure S9 shows that once the Ni(M)OOH is formed by electrochemical oxidation, it remains stable in the oxidized form even at the open circuit potential. The samples were subjected to the OER at 1.65 V for 20 min (Step III). During this time, the Raman spectra were recorded after 1, 5, 10, and 20 mins. For Ni and NiCo LDHs, the peaks of δ(Ni^{III}–O), ν(Ni^{III}–O), and ν(O–O) were immediately shifted back to the positions observed for the ^{16}O-labeled samples (Figure 3a,b). This result indicates that the ^{18}O-labeled lattice O and $NiOO^-$ moieties in the Ni and NiCo LDH are readily exchanged by ^{16}O atoms from $^{16}OH^-$ during the OER. It follows that lattice oxygen in Ni and NiCo LDHs participates in the OER process, similar to some recently reported perovskite catalysts.[8] The potential dependence of the oxygen exchange was probed (Figure S10). The exchange did not occur until a potential of 1.45 V, where the OER started to occur for Ni-based catalysts.[13] Thus, the lattice oxygen exchange in Ni and NiCo LDHs proceeds through the OER on the time scale of the Raman experiments.

As both O atoms of the $NiOO^-$ are exchanged with the O atoms from the electrolyte during the OER, a conceivable mechanism for this exchange is that the OO^- moiety is oxidized to dioxygen and leaves the Ni center, which can reform a $NiOO^-$ moiety with two hydroxide ions from the electrolyte. Thus, $NiOO^-$ is a precursor to dioxygen. The concentrations of $NiOO^-$ remained constant while the OER currents increased (Figure 1). It is possible that the $NiOO^-$ species are in a steady state so that their concentration is independent of the potential. However, we cannot rule out that an OER via a $NiOO^-$ precursor becomes a minor pathway at high overpotentials.

A strikingly different result was obtained for NiFe LDH. The δ(Ni^{III}–O), ν(Ni^{III}–O), and ν(O–O) peaks remained at their original frequencies during the OER (Figure 3c), with no evidence for ^{18}O-isotope exchange. This result indicates that lattice oxygen does not participate in the OER, in agreement with a recent study of $NiFeO_xH_y$ models derived from mass-selected NiFe nanoparticles.[9] It also suggests that $NiOO^-$ is not a precursor to dioxygen for NiFe LDHs. Thus, Fe incorporation completely changes the nature of the active site as well as the mechanism of the OER. To further corroborate this finding, similar isotope exchange and in situ Raman spectroscopic measurements were conducted on a NiCoFe LDH sample (20% Co and 5% Fe, Table S1 and Figures S11–S13). Incorporation of Fe into NiCo LDH also significantly increased its OER activity (Figure S11). Similar to NiFe LDH, no isotope exchange was observed for the δ(Ni^{III}–O), ν(Ni^{III}–O), and ν(O–O) bands in NiCoFe LDH (Figure S13). This result confirms the unique role of Fe in changing the active site and mechanism of the OER. The isotope-exchange experiments were repeated three times using independently prepared samples. The same spectroscopic behaviors were obtained.

Note that O-isotope exchange is possible for NiFe and NiCoFe LDHs in the first step of our procedure, but not for the second and third steps. The origin of this difference is probably the different states of the samples. In the first step, the samples exist in a Ni^{II} form as in $Ni(OH)_2$, which readily exchanges lattice O with OH^- in the solution. In the next steps, the samples are in the metastable state of NiOOH, which can only exchange lattice O through the OER. This fortuitous property makes it possible to reveal the role of Fe incorporation by the experiments described above. Three sets of experiments were conducted to test this hypothesis.

First, ^{16}O-labeled Ni, NiCo, and NiFe LDHs were first subjected to the OER at 1.65 V for 3 min, which converted the LDHs into NiOOH-type structures. Then the samples were placed in 0.1M Fe-free $H_2{}^{18}O$ solutions. For Ni and NiCo LDHs, ^{16}O exchange was observed for both Ni^{III}–O and

$NiOO^-$ moieties (Figure S14). However, no ^{16}O exchange occurred for NiFe LDH (Figure S14). This result supports our hypothesis that once NiFe LDH is converted into a Ni^{III} form, lattice O exchange can no longer occur.

Second, an ^{18}O-labeled NiFe LDH sample in the form of Ni^{III}, which did not exchange with $H_2{}^{16}O$ during the OER, was reduced to its Ni^{II} form. Then the sample was subjected to the OER at 1.65 V in a 0.1 M Fe-free $H_2{}^{16}O$ solution. Lattice oxygen exchange was then observed (Figure S15). This result further supports our hypothesis that oxygen exchange in the case of NiFe LDH depends on the oxidation state of Ni.

Third, the as-synthesized samples of the Ni, NiCo, and NiFe LDHs, where the Ni ions were in an oxidation state of +2, were subjected to oxygen exchange in the absence of an applied potential (Figure S16). Interestingly, lattice oxygen exchange was observed for all three catalysts. Thus, lattice oxygen exchange is facile for all the Ni-containing LDHs and requires no applied potential when the Ni ions are in the Ni^{II} form. However, once the Ni ions were oxidized to Ni^{III}, only Ni and NiCo LDHs were able to exchange their lattice O atoms through the OER, whereas the NiFe and NiCoFe LDHs could no longer exchange their lattice O atoms with the electrolyte.

The pH-dependence of the OER activity was investigated for Ni, NiCo, NiFe, and NiCoFe LDHs by LSV and chronoamperometric measurements in KOH solutions with different pH values (Figure S17 and S18).[5d,f,8,14] All four catalysts exhibit pH-dependent activity, consistent with literature results,[5d,f,14,15] although less pronounced than a recently reported NiFeCr catalyst.[16] This dependence indicates decoupled proton and electron-transfer steps in the catalytic cycle.[5f,8,14] A previous report on perovskite catalysts showed that only those in which lattice oxygen is used in the OER show pH-dependent activity.[8] Our result shows that pH dependence can also exist for catalysts involving no lattice oxygen, in agreement with the results obtained on mass-selected $NiFeO_xH_y$ models.[9] Thus, the correlation between pH dependence and lattice oxygen participation might not be universal.

Our results indicate that in the case of Ni and NiCo oxides, Ni sites in the bulk (coordinated by lattice oxygen atoms) are able to catalyze oxygen evolution, and $NiOO^-$ is a precursor to dioxygen. This precursor might be formed by the combination of two redox-active lattice oxygen atoms, or by OH^- attack of one such redox-active lattice oxygen atom (Figure 4a). When Fe is incorporated in these oxides, the OER occurs at a much lower overpotential and these Ni sites, while still present, are no longer the dominating active sites. A new surface site, highly active but invisible to Raman (this work) and many other spectroscopic techniques (e.g. XAS and Mössbauer),[5c,6a,c,d] is responsible for the observed activity of NiFe oxides. It is logical, although not proven by our results alone, that this site is a Fe site (Figure 4b).

In summary, by combining ^{18}O-labeling experiments with in situ Raman spectroscopy and using ultrathin LDH samples, we were able to obtain direct spectroscopic evidence for the different active sites in Fe-free and Fe-doped Ni oxides. In Fe-free Ni-containing oxides, bulk Ni sites are active and evolve oxygen via a $NiOO^-$ precursor. Lattice oxygen atoms participate in the reactions, probably through redox-active oxygen intermediates that form $NiOO^-$. Upon Fe incorporation, the catalytic activity is dramatically increased due to the creation of a new, highly reactive surface active site, mostly likely based on Fe. Lattice oxygen atoms no longer participate in the fast OER. Our findings reconcile conflicting observations in previous studies of Ni and NiFe oxides and provide a new mechanistic insight for NiFe oxide, the benchmark OER catalyst.

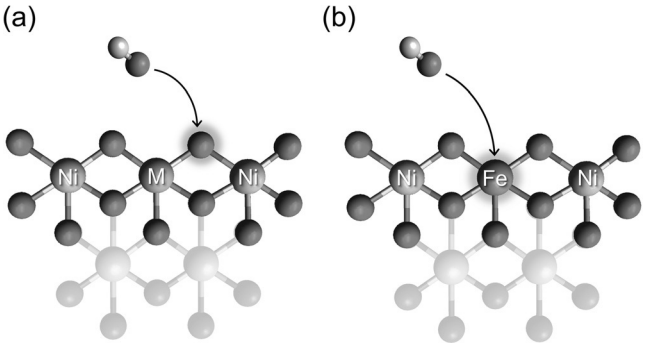

Figure 4. A model illustrating the different role of lattice oxygen in OER catalysis. a) Participation of lattice oxygen in Ni and NiCo LDHs. b) Nonparticipation of lattice oxygen on NiFe LDH. M = Ni or Co.

Acknowledgements

This work was supported by the European Research Council (no.681292) and the European Union's Horizon 2020 Research and Innovation Programme under grant agreement no. 732840 (A-LEAF). We thank Lichen Bai (EPFL) for help with TEM imaging.

Conflict of interest

The authors declare no conflict of interest.

Keywords: active site · electrocatalysis · nickel oxides · oxygen evolution reaction · Raman spectroscopy

How to cite: *Angew. Chem. Int. Ed.* **2019**, *58*, 10295 – 10299
Angew. Chem. **2019**, *131*, 10401 – 10405

[1] a) N. T. Suen, S. F. Hung, Q. Quan, N. Zhang, Y. J. Xu, H. M. Chen, *Chem. Soc. Rev.* **2017**, *46*, 337 – 365; b) F. Song, L. Bai, A. Moysiadou, S. Lee, C. Hu, L. Liardet, X. Hu, *J. Am. Chem. Soc.* **2018**, *140*, 7748 – 7759.

[2] a) Metal oxides are partially protonated in one or more states in the catalytic cycle of the OER. For example, nickel and nickel iron oxides exist as oxyhydroxides when the Ni ions are oxidized to +3 and higher oxidation states. For simplicity, we use the generic term of oxides to describe these catalysts; b) H. Bode, K. Dehmelt, J. Witte, *Electrochim. Acta* **1966**, *11*, 1079 – 1087; c) D. A. Corrigan, *J. Electrochem. Soc.* **1987**, *134*, 377 – 384; d) E. L. Miller, R. E. Rocheleau, *J. Electrochem. Soc.* **1997**, *144*, 3072 – 3077.

[3] a) M. W. Louie, A. T. Bell, *J. Am. Chem. Soc.* **2013**, *135*, 12329 – 12337; b) L. Trotochaud, S. L. Young, J. K. Ranney, S. W. Boettcher, *J. Am. Chem. Soc.* **2014**, *136*, 6744 – 6753.

[4] a) M. Gong, Y. Li, H. Wang, Y. Liang, J. Z. Wu, J. Zhou, J. Wang, T. Regier, F. Wei, H. Dai, *J. Am. Chem. Soc.* **2013**, *135*, 8452 – 8455; b) M. Gong, H. Dai, *Nano Res.* **2015**, *8*, 23 – 39; c) C. C. McCrory, S. Jung, J. C. Peters, T. F. Jaramillo, *J. Am. Chem. Soc.* **2013**, *135*, 16977 – 16987; d) F. Dionigi, P. Strasser, *Adv. Energy Mater.* **2016**, *6*, 1600621.

[5] a) M. S. Burke, L. J. Enman, A. S. Batchellor, S. Zou, S. W. Boettcher, *Chem. Mater.* **2015**, *27*, 7549 – 7558; b) S. Klaus, Y. Cai, M. W. Louie, L. Trotochaud, A. T. Bell, *J. Phys. Chem. C* **2015**, *119*, 7243 – 7254; c) D. Friebel, M. W. Louie, M. Bajdich, K. E. Sanwald, Y. Cai, A. M. Wise, M. J. Cheng, D. Sokaras, T. C. Weng, R. Alonso-Mori, R. C. Davis, J. R. Bargar, J. K. Norskov, A. Nilsson, A. T. Bell, *J. Am. Chem. Soc.* **2015**, *137*, 1305 – 1313; d) B. J. Trześniewski, O. Diaz-Morales, D. A. Vermaas, A. Longo, W. Bras, M. T. Koper, W. A. Smith, *J. Am. Chem. Soc.* **2015**, *137*, 15112 – 15121; e) M. Görlin, P. Chernev, J. Ferreira de Araújo, T. Reier, S. Dresp, B. Paul, R. Krahnert, H. Dau, P. Strasser, *J. Am. Chem. Soc.* **2016**, *138*, 5603 – 5614; f) M. Görlin, J. Ferreira de Araújo, H. Schmies, D. Bernsmeier, S. Dresp, M. Gliech, Z. Jusys, P. Chernev, R. Kraehnert, H. Dau, P. Strasser, *J. Am. Chem. Soc.* **2017**, *139*, 2070 – 2082; g) N. Li, D. K. Bediako, R. G. Hadt, D. Hayes, T. J. Kempa, F. Von Cube, D. C. Bell, L. X. Chen, D. G. Nocera, *Proc. Natl. Acad. Sci. USA* **2017**, *114*, 1486 – 1491; h) M. B. Stevens, C. D. Trang, L. J. Enman, J. Deng, S. W. Boettcher, *J. Am. Chem. Soc.* **2017**, *139*, 11361 – 11364.

[6] a) J. Y. Chen, L. Dang, H. Liang, W. Bi, J. B. Gerken, S. Jin, E. E. Alp, S. S. Stahl, *J. Am. Chem. Soc.* **2015**, *137*, 15090 – 15093; b) H. S. Ahn, A. J. Bard, *J. Am. Chem. Soc.* **2016**, *138*, 313 – 318; c) Z. K. Goldsmith, A. K. Harshan, J. B. Gerken, M. Vörös, G. Galli, S. S. Stahl, S. Hammes-Schiffer, *Proc. Natl. Acad. Sci. USA* **2017**, *114*, 3050 – 3055; d) B. M. Hunter, N. B. Thompson, A. M. Müller, G. R. Rossman, M. G. Hill, J. R. Winkler, H. B. Gray, *Joule* **2018**, *2*, 747 – 763.

[7] O. Diaz-Morales, D. Ferrus-Suspedra, M. T. M. Koper, *Chem. Sci.* **2016**, *7*, 2639 – 2645.

[8] A. Grimaud, O. Diaz-Morales, B. Han, W. T. Hong, Y. L. Lee, L. Giordano, K. A. Stoerzinger, M. T. M. Koper, Y. Shao-Horn, *Nat. Chem.* **2017**, *9*, 457 – 465.

[9] C. Roy, B. Sebok, S. B. Scott, E. M. Fiordaliso, J. E. Sørensen, A. Bodin, D. B. Trimarco, C. D. Damsgaard, P. C. K. Vesborg, O. Hansen, I. E. L. Stephens, J. Kibsgaard, I. Chorkendorff, *Nat. Catal.* **2018**, *1*, 820 – 829.

[10] J. Yu, B. R. Martin, A. Clearfield, Z. Luo, L. Sun, *Nanoscale* **2015**, *7*, 9448 – 9451.

[11] a) F. Song, X. Hu, *Nat. Commun.* **2014**, *5*, 4477; b) L. Han, S. Dong, E. Wang, *Adv. Mater.* **2016**, *28*, 9266 – 9291.

[12] M. Merrill, M. Worsley, A. Wittstock, J. Biener, M. Stadermann, *J. Electroanal. Chem.* **2014**, *717*, 177 – 188.

[13] R. D. Smith, C. P. Berlinguette, *J. Am. Chem. Soc.* **2016**, *138*, 1561 – 1567.

[14] C. Yang, O. Fontaine, J. M. Tarascon, A. Grimaud, *Angew. Chem. Int. Ed.* **2017**, *56*, 8652 – 8656; *Angew. Chem.* **2017**, *129*, 8778 – 8782.

[15] X. Lu, C. Zhao, *Nat. Commun.* **2015**, *6*, 6616.

[16] L. Fan, P. Zhang, B. Zhang, Q. Daniel, B. J. J. Timmer, F. Zhang, L. Sun, *ACS Energy Lett.* **2018**, *3*, 2865 – 2874.

Manuscript received: March 14, 2019
Revised manuscript received: May 1, 2019
Accepted manuscript online: May 20, 2019
Version of record online: June 17, 2019

